Structural characterization of folded pentapeptides containing centrally positioned β(R)Val, γ(R)Val and γ(S)Val residues

Article *in* Tetrahedron · June 2012

DOI: 10.1016/j.tet.2012.02.034

CITATIONS
9

READS
129

4 authors, including:

Dinesh Bhimareddy
French National Centre for Scientific Research
22 PUBLICATIONS **282** CITATIONS

SEE PROFILE

Krishnayan Basuroy
Deutsches Elektronen-Synchrotron
23 PUBLICATIONS **182** CITATIONS

SEE PROFILE

Padmanabhan Balaram
Indian Institute of Science
595 PUBLICATIONS **19,813** CITATIONS

SEE PROFILE

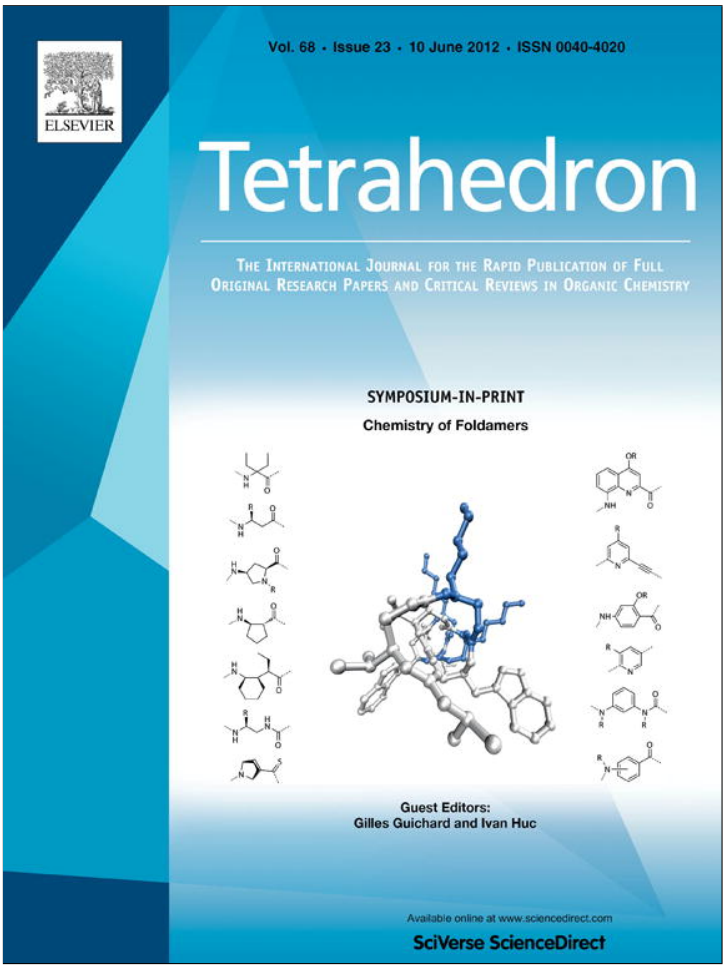

Tetrahedron 68 (2012) 4374–4380

Contents lists available at SciVerse ScienceDirect

Tetrahedron

journal homepage: www.elsevier.com/locate/tet

Structural characterization of folded pentapeptides containing centrally positioned β(*R*)Val, γ(*R*)Val and γ(*S*)Val residues

Bhimareddy Dinesh [a], Krishnayan Basuroy [b], Narayanaswamy Shamala [b,*], Padmanabhan Balaram [a,*]

[a] *Molecular Biophysics Unit, Indian Institute of Science, Bangalore 560012, India*
[b] *Department of Physics, Indian Institute of Science, Bangalore 560012, India*

ARTICLE INFO

Article history:
Received 27 October 2011
Received in revised form 11 February 2012
Accepted 14 February 2012
Available online 18 February 2012

Keywords:
β and γ Amino acids
Hybrid peptides
Backbone expanded helix
Peptide conformation
Crystal structures

ABSTRACT

A cylindrical pore of ~7.5 Å diameter containing a one-dimensional water wire, within the confines of a hydrophobic channel lined with the valine side chain, has been observed in crystals of the peptide Boc–D-Pro-Aib-Val-Aib-Val–OMe (**1**) (Raghavender et al., 2009, 2010). The synthesis and structural characterization in crystals of three backbone homologated analogues Boc–D-Pro-Aib-β^3(*R*)Val-Aib-Val–OMe (**2**), Boc–D-Pro-Aib-γ^4(*R*)Val-Aib-Val–OMe (**3**), Boc–D-Pro-Aib-γ^4(*S*)Val-Aib-Val–OMe (**4**) are described. Crystal structures of peptides **2**, **3** and **4** reveal close-packed arrangements in which no pore was formed. In peptides **2** and **3** the N-terminus D-Pro-Aib segment adopted conformations closely related to Type II′ β-turns, while residues 2–4 form one turn of an αβ right-handed C_{11} helix in **2** and an αγ C_{12} helix in **3**. In peptide **4**, a continuous left-handed helical structure was observed with the D-Pro-Aib segment forming a Type III′ β-turn, followed by one turn of a left-handed αγ C_{12} helix.

1. Introduction

The serendipitous observation that the peptide Boc–D-Pro-Aib-Leu-Aib-Val–OMe, formed a tubular structure in crystals, enclosing an empty pore of ~5.2 Å diameter, prompted us to investigate the analogue Boc–D-Pro-Aib-Val-Aib-Val–OMe (**1**). The peptide **1** crystallized in space group $P6_5$, with a cylindrical pore of ~7.5 Å diameter, coincident with the 6-fold screw axis. The channel, thus formed, had a completely hydrophobic lining encapsulating a wire of water molecules, which did not have any hydrogen bond interaction with the channel walls. The Val(3) residue is a part of the inner lining of the pore, with its isopropyl side chain protruding into the interior of the channel (Fig. 1a and b).[1]

A subsequent study of the pentapeptides Boc–D-Pro-Aib-Xxx-Aib-Val–OMe [Xxx=Ala, Phe], revealed that the hydrophobic pore encapsulating the water wire was observed only in the case of Xxx=Val (**1**).[2] Crystal structure determination of four pentapeptides of this series, together with four independent enantiomers, established that this sequence consistently adopts a well-defined backbone conformation, stabilized by three intramolecular hydrogen bonds (Fig. 1c). The D-Pro-Aib segment forms a Type II′ β-turn structure followed by two successive Type I/III β-turn conformations over the segment Aib(2)-Xxx(3)-Aib(4). Residues 2, 3 and 4 adopt right-handed helical (α_R) conformations. These observations suggested that the nature and precise positioning of the residue 3 side chain was critical for the formation of porous crystals, with hydrophobic channels, since variation of the residue 3 side chain appeared to abolish pore formation, with the exception of LVal and LLeu. We therefore turned to exploring this effect of backbone variation[3] on the molecular conformation and crystal packing in this peptide series. Stimulated by the growing interest in the structural chemistry of peptides containing β and γ amino acid residues,[4] we synthesized the following analogues of peptide (**1**), Boc–D-Pro-Aib-β^3(*R*)Val-Aib-Val–OMe (**2**), Boc–D-Pro-Aib-γ^4(*R*)Val-Aib-Val–OMe (**3**), Boc–D-Pro-Aib-γ^4(*S*)Val-Aib-Val–OMe (**4**).[†]

Crystallographic characterization of peptides **2**–**4**, described in this report establish that well folded structures stabilized by intramolecular hydrogen bonds are indeed formed in the cases of backbone expanded peptide analogues. However, the crystals

* Corresponding authors. Tel.: +91 80 2360 2741; fax: +91 80 2360 0535 (P.B.); tel.: +91 80 2360 2602; fax: +91 80 2293 2856 (N.S.); e-mail addresses: shamala@physics.iisc.ernet.in (N. Shamala), pb@mbu.iisc.ernet.in (P. Balaram).

† Note: Boc–β(*R*)Val–OH and Boc–γ(*R*)Val–OH are formed by homologation of Boc–L-Val–OH (Boc–*S*-Val–OH). Note the change in absolute configuration. The abbreviations follow Seebach et al. (2004).[4a]

0040-4020/$ – see front matter © 2012 Elsevier Ltd. All rights reserved.
doi:10.1016/j.tet.2012.02.034

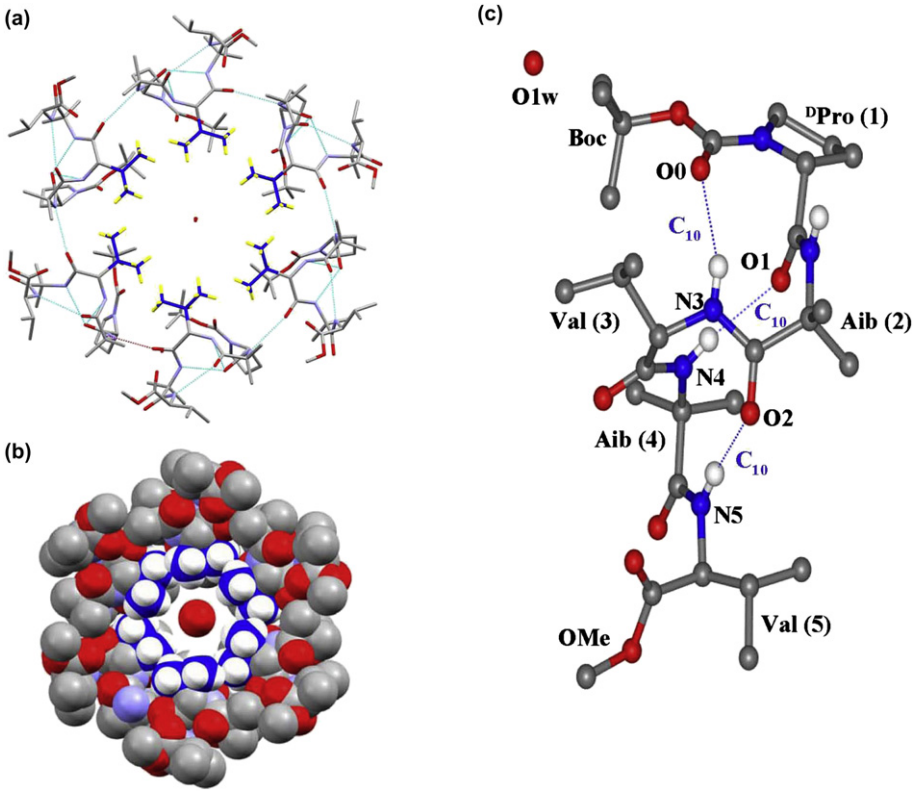

Fig. 1. (a) View down the hydrophobic channels formed in the crystal structure of Boc–D-Pro-Aib-Val-Aib-Val–OMe (**1**). The isopropyl groups of Val(3) side chain are highlighted. (b) Space filling view of the hydrophobic channel enclosing a water wire hydrogen atoms (white) are shown only for the Val(3) side chain. (c) Molecular conformation of peptide **1**, Type II′ β-turn followed by two consecutive right-handed 3_{10} turns.

formed reveal close-packed structures, with the absence of hydrophobic pores.

2. Results and discussion

Single crystals suitable for X-ray diffraction were obtained for peptides **2**, **3** and **4**. In the case of peptide **3** [Boc–D-Pro-Aib-γ^4(*R*)Val-Aib-Val–OMe], two different polymorphic forms were obtained and the structures determined in both the cases. Table 1 summarises the backbone torsional parameters for peptides **2**–**4**. Corresponding values for the parent peptide **1** are also summarised. Table 2 summarises hydrogen bond parameters in the crystal structures of peptides **2**–**4**. In all cases, the molecules crystallized in a close-packed fashion, in contrast to the case of **1**, where crystals with large pores were formed (Fig. 1a and b). The effect of insertion of backbone homologated residues on the folded structures of the peptides is considered below.

2.1. Molecular conformations of peptides

In crystals, peptide **2** [Boc–D-Pro-Aib-β^3(*R*)Val-Aib-Val–OMe] crystallized in the monoclinic space group $P2_1$, with four independent molecules in the asymmetric unit named A, B, C, D. The backbone conformation of two of these molecules, A and B are illustrated in Fig. 2. Inspection of the backbone torsion angles and hydrogen bond parameters (Tables 1 and 2), establishes that in molecule A the Aib(2)-β^3(*R*)Val(3)-Aib(4) segment is stabilized by two consecutive C_{11} hydrogen bonds. The consecutively formed hybrid αβ turns[5] correspond to a short stretch of a right-handed 3_{10} helical structure, expanded by the insertion of a additional methylene group in the backbone at residue 3. In molecule B, three intramolecular hydrogen bonds are observed, with an additional C_{10} hydrogen bond stabilizing a Type II′ β-turn conformation for the D-Pro(1)-Aib(2) segment. The main conformational difference between molecule A and molecule B is observed at the N-terminus,

Table 1
Backbone torsion angles for peptides **1**–**4**[a]

	D-Pro(1)		Aib(2)		Xxx(3)				Aib(4)		Val(5)	
	ϕ (°)	ψ (°)	ϕ (°)	ψ (°)	ϕ (°)	θ_1 (°)	θ_2 (°)	ψ (°)	ϕ (°)	ψ (°)	ϕ (°)	ψ (°)
Peptide **1**	53.9	−137.0	−59.6	−24.2	−73.9			−1.2	−55.4	−31.6	−85.7	130.3
Peptide **2**												
Molecule A	63.8	−162.2	−56.2	−43.3	−102.7		98.3	−79.3	−57.3	−39.3	−100.9	−62.7
Molecule B	50.0	−144.1	−60.3	−28.7	−113.7		79.8	−68.4	−54.4	−39.5	−113.7	−21.9
Molecule C	48.1	−142.7	−64.6	−25.4	−107.1		76.8	−69.7	−53.9	−42.2	−116.5	−4.14
Molecule D	63.8	−160.4	−55.1	−46.3	−99.1		94.5	−80.2	−57.8	−38.1	−103.4	−55.3
Peptide **3a**	72.4	−162.8	−59.3	−42.5	−127.8	50.1	61.1	−116.1	−58.9	−41.1	−127.5	177.0
Peptide **3b**	65.9	−165.5	−64.2	−48.1	−129.7	50.5	62.2	−114.0	−58.5	−42.0	−130.0	165.6
Peptide **4**	61.7	21.8	56.2	30.2	124.8	−48.0	−64.2	111.9	61.3	32.3	−68.1	141.5

[a] Values for 1 are from Ref. 1.

Table 2
Hydrogen bond parameters in the crystal structures of peptides **2**–**4**

Donor	Acceptor	D···A (Å)	H···A (Å)	D–H···A (°)
Peptide 2				
Intramolecular				
Molecule A				
N4	O1	2.968	2.120	168.95
N5	O2	2.891	2.079	157.18
Molecule B				
N3	O0	3.346	2.666	136.91
N4	O1	3.172	2.358	158.03
N5	O2	3.111	2.262	169.14
Molecule C				
N3	O0	3.323	2.667	134.10
N4	O1	3.142	2.328	157.99
N5	O2	3.077	2.233	167.17
Molecule D				
N4	O1	2.882	2.034	168.37
N5	O2	2.925	2.100	160.51
Intermolecular				
N3—A	O4[a]—C	3.010	2.186	160.52
N2—B	O4[b]—D	2.943	2.194	145.40
N2—C	O4[c]—A	3.008	2.253	146.52
N3—D	O4[c]—B	3.059	2.224	163.68
Solvent mediated hydrogen bonds				
N2—**A**	O1W	2.913	2.064	168.92
O1W	O3[c]—A	2.858		
O1W	O3[a]—C	2.866		
O2W	O3—B	2.868		
O2W	O3—D	2.897		
N2—D	O2W[c]	2.854	2.006	168.79
Peptide 3a				
Intramolecular				
N4	O1	2.908	2.050	174.28
N5	O2	2.950	2.065	167.71
Intermolecular				
N2	O3[d]	2.853	1.968	170.22
Solvent mediated hydrogen bonds				
O1w	O0	2.852	1.929	164.47
N3	O1w	2.919	2.067	161.41
O1w	O4[d]	2.828	1.954	150.36
Peptide 3b				
Intramolecular				
N4	O1	2.935	2.121	165.59
N5	O2	3.117	2.292	166.37
Intermolecular				
N3	O4[d]	2.956	2.136	162.65
Solvent mediated hydrogen bonds				
N2	O1E	2.912	2.079	174.95
O1E	O3[d]	2.753	2.139	131.70
Peptide 4				
Intramolecular				
N3	O0	3.000	2.154	163.13
N4	O1	2.966	2.073	167.91
N5	O2	2.931	2.088	166.84
Intermolecular				
N2	O3[c]	3.055	2.299	147.56

[a] Translation related by $x, y, z-1$.
[b] Translation related by $x, y, z+1$.
[c] Translation related by $x-1, y, z$.
[d] Symmetry related by $-x, y-1/2, -z+1/2$.

with D-Pro(1) adopting a ψ value ($\psi \sim -160°$, molecules A, D; $\psi \sim -140°$, molecules B, C), which deviates significantly from that expected in an ideal Type II′ β-turn ($\psi = -120°$). Molecules A and D in the asymmetric unit of peptide **2** adopt very similar conformations, while molecules B and C are conformationally similar. Two co-crystallized water molecules are observed in the asymmetric unit of peptide **2**.

The observed distortion at the N-terminus in the case of molecules A and D, is a consequence of an intermolecular hydrogen bond formed between (*R*)β^{3}Val(3)NH of molecule A and Aib(4) C=O of molecule C of translated asymmetric unit along the *z*-axis (Fig. 3).

Depending on the crystallization conditions, peptide **3** crystallized in two polymorphic forms, both of which were orthorhombic ($P2_12_12_1$). In one case a co-crystallized water molecule was observed, while in the other a molecule of ethanol was obtained (Fig. 4). Both molecules adopted a very similar backbone conformations, with two consecutive αγ C_{12} turns being formed at the Aib(2)-γ^4(*R*)Val(3)-Aib(4) segment. The torsion angles and the hydrogen-bonding pattern correspond to one turn of a right-handed αγ C_{12} helix, which is a backbone expanded analogue of the classical 3_{10} helix.[5b,6] Torsion angles at the N-terminus D-Pro(1)-Aib(2) segment deviate considerably from the values expected for ideal Type II′ β-turns. Consequently, the C_{10} hydrogen bond Boc(0) CO···HNγ^4(*R*)Val (3) is not formed. The overall backbone fold for the two independent molecules of peptide **3** is very similar to that obtained for molecules A and D in peptide **2**. Comparison of peptides **2** and **3** with the parent peptide **1** establishes that the right-handed helical turn formed by the Aib(2)-Xxx(3)-Aib(4) segment is maintained, despite the expansion of the backbone at residue 3.

Peptide **4** [Boc–D-Pro-Aib-γ^4(*S*)Val-Aib-Val–OMe] crystallized in the triclinic space group *P*1. The molecular conformation is shown in Fig. 5. Three intramolecular hydrogen bonds, C_{10}, C_{12} and C_{12} stabilized the folded structure. Inspection of the torsion angles in Table 1 established that the molecule folds into a left-handed helix, with the Type III′ β-turn at the D-Pro(1)-Aib(2) segment followed by two consecutive αγ C_{12} turns. Such hybrid helical hydrogen bonding patterns are observed in peptides containing both α residues and higher homologues.[5–7] An interesting feature of peptide **4** is the switching of the turn type at the N-terminus D-Pro(1)-Aib(2) segment. While this segment adopted conformations very close to that Type II′ β-turns in all the other examples, an almost ideal Type III′ β-turn is observed in peptide **4**.

2.2. Circular dichroism (CD)

Fig. 6 shows the far-UV CD spectra of the pentapeptides containing a central γ-valine residue at position 3 (**3**, γ^4(*R*)Val; **4**, γ^4(*S*)Val). In the case of peptide **3** (γ^4(*R*)Val) a negative band is observed at ~215 nm. In contrast, for peptide **4** (γ^4(*S*)Val) a positive band is observed at ~215 nm, with a crossover point at ~203 nm. This is consistent with the X-ray diffraction results where a change in the handedness of the short helical fold is observed. In peptide **3** the N-terminus Type II′ β turn is followed by a *right-handed* αγ helix, while in peptide **4**, a *left-handed* helical fold encompassing both the Type I′ β turn segment and the two successive αγ C_{12} turns is observed. While a detailed interpretation of CD spectra for short hybrid sequences may be premature, it is clear that the sense of twist of the helical backbone observed in crystals is indeed maintained in solution.

3. Conclusions

The structural results presented above for peptides **2** and **3** suggest that insertion of an additional methylene groups at the central position in this series of pentapeptides does not disrupt the folded, intramolecularly hydrogen bonded structure. The change of chirality at position 3 results a switch in the handedness of the helix in peptide **4**. The β-amino acid residue in peptide **2** adopts an approximately *gauche* conformation about the C^α–C^β bond. In peptides **3** and **4**, the centrally positioned γ-amino acid residue adopts a *gauche* conformation about the C^α–C^β and C^β–C^γ bonds. The tendency of β and γ residues bearing backbone substituents to adopt locally compact conformations, facilitates their incorporation into helical peptide backbones. While foldamer design has often focussed on studies of more severely constrained β and γ residues,[8] it is clear that residues readily accessible, synthetically, from chiral α amino acid residues can also be used in the design of folded

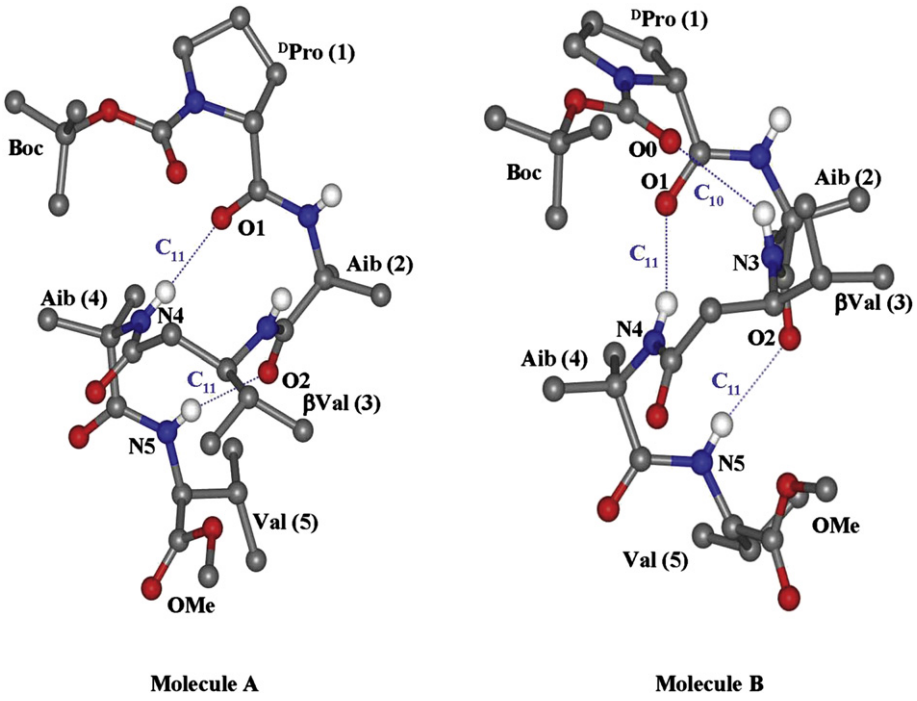

Fig. 2. Conformations of two independent molecules A and B in peptide Boc–D-Pro-Aib-β^3(*R*)Val-Aib-Val–OMe (**2**). The asymmetric unit contains four independent molecules (A, B, C, D). The pairs A, D and B, C have similar conformations.

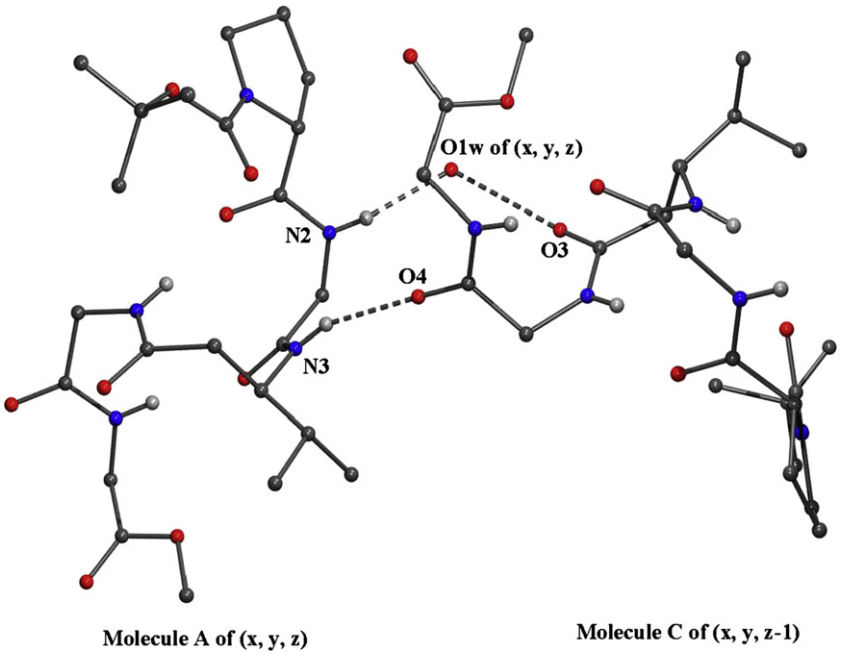

Fig. 3. A view of the intermolecular interaction observed between molecules A and a translated molecule C in crystals of peptide Boc–D-Pro-Aib-β^3(*R*)Val-Aib-Val–OMe (**2**).

peptides, which mimic conformational features characterized in sequences comprising exclusively of α-amino acid residues.

4. Experimental

4.1. General

All reagents were purchased from commercial sources and were used without further purification. Melting points were determined using Stuart melting point apparatus SMP10. Electrospray ionization mass spectrometry (ESI-MS) was done on a Bruker Daltonics Esquire-3000 instrument. Far-UV circular dichroism (CD) spectra were recorded on a JASCO J-715 spectropolarimeter. X-ray data were collected on Bruker AXS KAPPA APEXII CCD with MoKα (λ=0.71073 Å) radiation and Bruker AXS ULTRA APEXII CCD (rotating anode X-ray generator) with Cuk$_\alpha$ (λ=1.54178 Å) radiation. ^{1}H NMR spectra were recorded on Bruker 500-MHz or 700-MHz spectrometers. Chemical shifts were measured in delta with TMS or residual solvent signal as a standard.

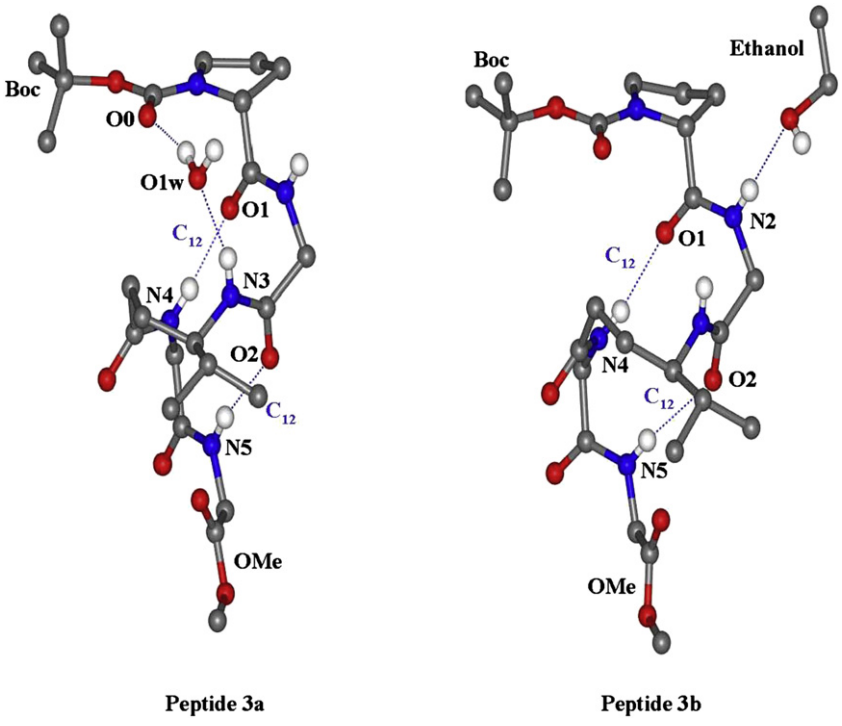

Fig. 4. Conformations in crystals of peptide Boc–D-Pro-Aib-γ^4(*R*)Val-Aib-Val–OMe (**3**) in two polymorphic crystals **3a** and **3b**.

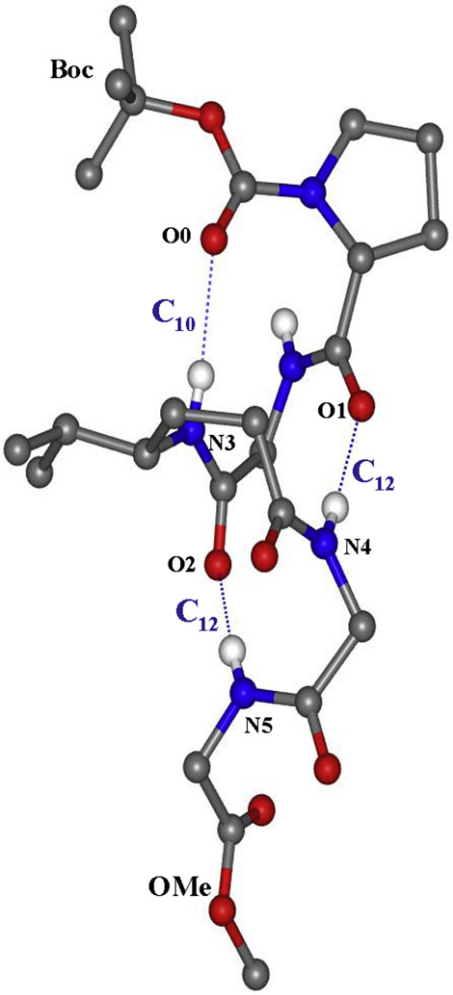

Fig. 5. Conformation in crystals of peptide Boc–D-Pro-Aib-γ^4(*S*)Val-Aib-Val–OMe (**4**).

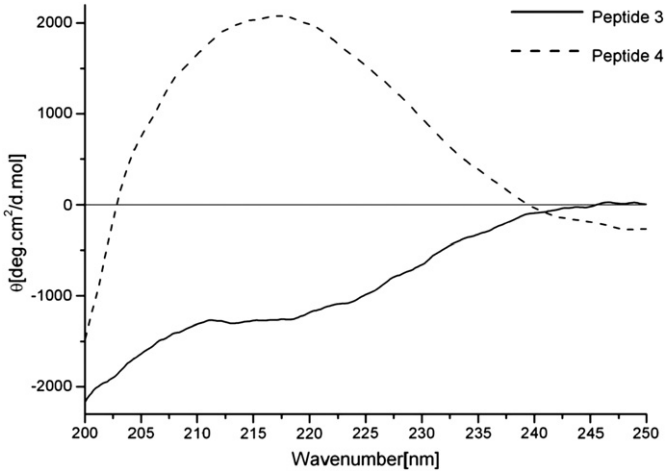

Fig. 6. A comparison of the CD spectra of peptides Boc–D-Pro-Aib-γ^4(*R*)Val-Aib-Val–OMe (**3**) and Boc–D-Pro-Aib-γ^4(*S*)Val-Aib-Val–OMe (**4**) in methanol.

4.2. Synthesis of β^3(*R*)-valine

Literature procedures[9,10] were followed with minor modifications. Briefly, Boc–L-Val–OH (10 mmol) was dissolved in anhydrous tetrahydrofuran (THF, 25 ml) and then cooled to −15 °C. Triethylamine (Et_3N, 1.25 ml, 1 equiv) and ethyl chloroformate ($ClCO_2Et$, 1.25 ml, 1 equiv) were added to the solution. After 30 min, the triethylamine salt was filtered off and the filtrate was cooled to ~−15 °C. The cooled filtrate was charged with diazomethane (CH_2N_2) until a rich greenish-yellow colour persisted. The mixture was then stirred for 5 h. After aqueous workup by successive washing with 10% $KHSO_4$ (3×50 ml), 5% $NaHCO_3$ (3×50 ml) and brine (30 ml), the organic layer was dried over Na_2SO_4 and concentrated under reduced pressure. The crude product was subjected to Wolff rearrangement as previously described.[11] The diazoketone (10 mmol) was dissolved in THF (25 ml) with the

addition of 10% (v/v) H_2O and then cooled to ~−15 °C. A solution of silver acetate (1 mmol) in Et_3N (11 mmol) was added, and the resulting mixture stirred for 3 h. The progress of the reaction was monitored by TLC ($CHCl_3$/MeOH/AcOH 40:2:1 (v/v)). The solvent was removed under reduced pressure and diluted with H_2O. The aqueous phase was extracted with ethyl acetate (AcOEt), and the resulting colourless aqueous phase was adjusted to pH 2 with 50% $KHSO_4$ and extracted with AcOEt. The AcOEt extracts were washed with brine, dried (Na_2SO_4) and the solvent was removed under reduced pressure to obtain Boc–β^3(*R*)-Val (yield ~60%). ^{1}H NMR, δ ppm (700 MHz, $CDCl_3$): 0.93 (d, 6H, $C^{\delta}H_3$), 1.50 (s, 9H, Boc CH_3), 1.85 (m, 1H, $C^{\gamma}H$), 2.55 (d, 2H, $C^{\alpha}H_2$), 3.75 (m, 1H, $C^{\beta}H$), 4.92 (d, 1H, NH).

4.3. Synthesis of γ^4(*R*) and γ^4(*S*)-valine

A previously described procedure[12] was used with minor modification.

Step 1. Boc–L-Val–OH or Boc–D-Val–OH (20.2 g, 93 mmol) was dissolved with 2,2-dimethyl-1,3-dioxane-4,6-dione[12] (Meldrum's acid, 14.7 g, 102.3 mmol) and 4-dimethylaminopyridine (DMAP, 17 g, 139.5 mmol) in 200 ml of CH_2Cl_2. The reaction mixture was cooled to 0 °C and a solution of *N*,*N*′-dicyclohexylcarbodiimide (DCC, 21 g, 102.3 mmol) in 100 ml of CH_2Cl_2 was added dropwise. The mixture was then stirred for about 2 h at room temperature and kept in the refrigerator, overnight. The precipitated dicyclohexyl urea was filtered off, washed with 10% $KHSO_4$, brine and dried over anhydrous Na_2SO_4. The solution was used for the next step without purification.

Step 2. To the cooled solution from step 1, 98% acetic acid (61 ml, 1023 mmol) was added. The reaction mixture was allowed to cool, $NaBH_4$ (8.8 g, 232 mmol) added in small portions with stirring over 1.5 h. The reaction mixture was left in the refrigerator overnight. Workup was by successive washing with 5% $KHSO_4$ (2×), brine (2×) and water (2×). The organic layer was dried over anhydrous Na_2SO_4 and evaporated to dryness. The obtained product was passed through a 150 g pad of silica gel (60–120 mesh) with 1:1 AcOEt/petroleum ether mobile phase. The recovered solid was stirred with petroleum ether for about 20 min. and filtered through sintered glass funnel to obtain a fine powder.

Step 3. The product from the previous step was refluxed in 150 ml of toluene for about 3.5 h. The solvent was removed under reduced pressure to obtain a cyclized pyrrolidinone product.

Step 4. The pyrrolidinone (12–14 g, ~50 mmol) dissolved in 25:35 acetone/water was cooled in an ice bath, NaOH (4–5 g) added and stirred for 30 min. Acetone was removed under reduced pressure and the aqueous solution was acidified with 25% $KHSO_4$ to pH 2. The precipitated solid was filtered and washed with water to get pure corresponding Boc–γ^4(*R*)-Val–OH or Boc–γ^4(*S*)-Val–OH (yields ~75%). ^{1}H NMR δ ppm (700 MHz, $CDCl_3$): 0.89–0.92 (d, 6H, $C^{\varepsilon}H_3$), 1.45 (s, 9H, Boc CH_3), 1.55–1.88 (m, 3H, $C^{\delta}H_2$, $C^{\beta}H$), 2.4 (m, 2H, $C^{\alpha}H_2$), 3.4 (m, 1H, $C^{\gamma}H$), 4.36, 5.81 (d, 1H, NH).

4.4. Peptide synthesis

Peptides **2**, **3** and **4** were synthesized by conventional solution-phase methods, by means of a fragment condensation strategy. The Boc-group was used for N-terminal protection, and the C-terminus was protected as a methyl ester. Deprotections (monitored by TLC) were performed with 98–100% formic acid (HCOOH) and saponification for the N- and C-terminal protecting groups, respectively. Couplings were mediated by 1-[3-(dimethylamino)propyl]-3-ethylcarbodiimide hydrochloride (EDC) and 1-hydroxy-1*H*-benzotriazole (HOBt) (1.01 equiv.). The final peptide Boc–D-Pro-Aib-Xxx-Aib-Val–OMe (Xxx=β^3(*R*)Val, γ^4(*R*)Val, γ^4(*S*)Val) was achieved by fragment condensation of Boc–D-Pro-Aib–OH with H_2N–Xxx-Aib-Val–OMe. All the intermediates were characterized by electrospray ionization mass spectrometry (ESI-MS), 500/700-MHz ^{1}H NMR and thin-layer chromatography (TLC) on silica gel (SiO_2, $CHCl_3$/MeOH 9:1 (v/v)) and were used without further purification. The final peptides were obtained as pure products after washing with hexane/ether mixtures. The peptides were characterized by ESI-MS and by 700-MHz ^{1}H NMR spectra. Far-UV circular dichroism (CD) spectra (Fig. 6) were recorded for peptides **3** and **4** with methanol as the solvent. A path length of 1 mm was used. Data were acquired in the wavelength-scan mode by using a 1 nm bandwidth with a step size of 0.2 nm and a scan speed of 10 nm min^{-1}. Typically, two scans were acquired, and the data were averaged. Solvent subtraction was carried out by using methanol as a blank, and the spectra were smoothened. Mass spectral data (*m*/*z*): peptides **2**, 612.3 $[M+H]^+$ (*M*cal) 611.7 Da, 634.3 $[M+Na]^+$, 650.3 $[M+K]^+$; **3** and **4**, 626.3 $[M+H]^+$ (*M*cal) 625.8 Da, 648.3 $[M+Na]^+$, 664.3 $[M+K]^+$. Melting points (°C): peptides **2**, 154–156 °C; **3**, 115–117 °C and **4**, 172–173 °C. ^{1}H NMR, δ ppm (700 MHz, $CDCl_3$): Boc–D-Pro-Aib-β^3(*R*)Val-Aib-Val–OMe (**2**), 0.92/0.95/0.98 (12H, d, β^3(*R*)Val $C^{\delta}H_3$, Val $C^{\gamma}H_3$), 1.48 (9H, s, Boc CH_3), 1.50/1.63 (12H, s, Aib $C^{\beta}H_3$), 1.87/2.24 (4H, m, D-Pro $C^{\beta}H_2$/$C^{\gamma}H_2$), 2.38 (2H, d, β^3(*R*)Val $C^{\alpha}H_2$) 3.43 (2H, d, D-Pro $C^{\delta}H_2$), 3.7 (3H, s, OCH_3), 4.05 (1H, br, β^3(*R*)Val $C^{\beta}H$), 4.11 (1H, t, D-Pro $C^{\alpha}H$), 4.46 (1H, q, Val $C^{\alpha}H$), 6.8 (1H, s, Aib NH), 6.96 (1H, br, β^3(*R*)Val NH), 7.28 (1H, s, Aib NH), 7.66 (1H, d, Val NH); Boc–D-Pro-Aib-γ^4(*R*)Val-Aib-Val–OMe (**3**), 0.88/0.9/0.94 (12H, d, γ^4(*R*)Val $C^{\varepsilon}H_3$, Val $C^{\delta}H_3$), 1.4 (γ^4(*R*)Val $C^{\alpha}H_3$), 1.46 (9H, s, Boc CH_3), 1.49/1.55 (12H, s, Aib $C^{\beta}H_3$), 1.88–2.05 (4H, m, D-Pro $C^{\beta}H_2$/$C^{\gamma}H_2$, 1H, γ^4(*R*)Val $C^{\delta}H$), 2.1 (2H, m, γ^4(*R*)Val $C^{\beta}H_2$), 3.43 (2H, br, D-Pro $C^{\delta}H_2$), 3.69 (3H, s, OCH_3), 3.84 (1H, m, γ^4(*R*)Val $C^{\gamma}H$), 4.1 (1H, br, D-Pro $C^{\alpha}H$), 4.48 (1H, q, Val $C^{\alpha}H$), 6.26 (1H, br, γ^4(*R*)Val NH), 6.79 (1H, br, Aib NH), 7.03 (1H, s, Aib NH), 7.88 (1H, br, Val NH); Boc–D-Pro-Aib-γ^4(*S*)Val-Aib-Val–OMe (**4**), 0.85/0.89/0.97 (12H, d, γ^4(*R*)Val $C^{\varepsilon}H_3$, Val $C^{\delta}H_3$), 1.49 (9H, s, Boc CH_3), 1.49/1.55 (12H, s, Aib $C^{\beta}H_3$), 1.89–2.08 (4H, m, D-Pro $C^{\beta}H_2$/$C^{\gamma}H_2$, 1H, γ^4(*S*)Val $C^{\delta}H$), 2.1 (2H, m, γ^4(*S*)Val $C^{\beta}H_2$), 3.49–3.58 (2H, m, D-Pro $C^{\delta}H_2$, 1H, γ^4(*R*)Val $C^{\gamma}H$), 3.72 (3H, s, OCH_3), 4.08 (1H, br, D-Pro $C^{\alpha}H$), 4.45 (1H, q, Val $C^{\alpha}H$), 6.36 (1H, s, Aib_2 NH), 6.72 (1H, d, γ^4(*S*)Val NH), 7.17 (1H, s, Aib_4 NH), 7.96 (1H, d, Val NH).

4.5. X-ray diffraction

Single crystals of the pentapeptides **2**, **3** and **4** were obtained by slow evaporation using a range of solvent conditions. Colourless single crystals were grown by dissolving ~8 mg of peptides **2**, **3a**, **3b** and **4** in acetone/water mixture (200 μl/ 10 μl), in ethyl acetate/petroleum ether mixture (100 μl/100 μl), in ethanol (300 μl) and in ether (500 μl), respectively. Peptide **2** crystallized in the monoclinic space group $P2_1$, with four peptide molecules and two co-crystallized water molecules in the asymmetric unit. For peptide **3**, polymorphic forms (ethyl acetate/petroleum ether and ethanol) were obtained. Form **3a** crystallized with one peptide molecule and one water molecule in the asymmetric unit. Form **3b** crystallized with one peptide molecule and one ethanol molecule in the asymmetric unit. Forms **3a** and **3b** both crystallized in the same orthorhombic space group $P2_12_12_1$, whereas peptide **4** crystallized in the triclinic space group *P*1, without any co-crystallizing solvent.

For peptides **2** and **4**, X-ray data were collected on Bruker AXS KAPPA APEXII CCD with MoKα (λ=0.71073 Å) radiation and for peptides **3a** and **3b** X-ray data were collected on Bruker AXS ULTRA APEXII CCD (rotating anode X-ray generator) with CuKα (λ=1.54178 Å) radiation. These data sets were collected in phi and omega scan type mode. For peptides **2** and **4**, the structures were solved by using iterative dual space direct methods in SHELXD[13] and for peptides **3a** and **3b**, the structures were solved by direct methods in SHELXS.[14] After the initial solution methods all the structures were refined against F^2 isotropically followed by full

matrix anisotropic least-squares refinement using SHELXL-97.[15] The solvent molecules in peptides **2**, **3a** and **3b** were located from difference Fourier maps. For peptide **2**, all the hydrogen atoms were fixed geometrically in idealized positions and allowed to ride with the C or N atom to which each was bonded, in the final cycles of refinement. The hydrogen atoms of the co-crystallized water molecules in peptide **2** could not be located from the difference Fourier map. In the case of peptides **3a**, **3b** and **4** all the hydrogen atoms attached to N atoms and hydrogen atoms bonded to some other C atoms also were located from the difference Fourier map and suitable restraints were applied judiciously in order to get a chemically meaningful geometry.

The final R value for peptide **2** was R_1=0.0770 (wR_2=0.2403) for 6858 observed reflections with $F_o \geq 4\sigma|F_o|$ and for 1568 parameters. The final R value for peptide **3a** was R_1=0.0472 (wR_2=0.1509) for 3790 observed reflections with $F_o \geq 4\sigma|F_o|$ and for 458 parameters. The final R value for peptide **3b** was R_1=0.0450 (wR_2=0.1409) for 3634 observed reflections with $F_o \geq 4\sigma|F_o|$ and for 490 parameters. The final R value for peptide **4** was R_1=0.0507 (wR_2=0.1467) for 3251 observed reflections with $F_o \geq 4\sigma|F_o|$ and for 490 parameters. CCDC deposition numbers for the peptides are 848245 (**2**), 848246 (**3a**), 848247 (**3b**) and 848248 (**4**).

Acknowledgements

This work is supported by a program grant from the Department of Biotechnology (DBT), India, in the area of Molecular Diversity and Design. B.D. is supported by the award of an UGC-DSK Postdoctoral Fellowship from the University Grants Commission (UGC), India.

References and notes

1. Raghavender, U. S.; Aravinda, S.; Shamala, N.; Kantharaju; Rai, R. K.; Balaram, P. *J. Am. Chem. Soc.* **2009**, *131*, 15130–15132.
2. Raghavender, U. S.; Kantharaju; Aravinda, S.; Shamala, N.; Balaram, P. *J. Am. Chem. Soc.* **2010**, *132*, 1075–1086.
3. Karle, I. L.; Pramanik, A.; Banerjee, A.; Bhattacharjya, S.; Balaram, P. *J. Am. Chem. Soc.* **1997**, *119*, 9087–9095.
4. (a) Seebach, D.; Beck, A. K.; Bierbaum, D. J. *Chem. Biodivers.* **2004**, *1*, 1111–1239; (b) Gellman, S. H. *Acc. Chem. Res.* **1998**, *31*, 173–180; (c) Cheng, R. P.; Gellman, S. H.; DeGrado, W. F. *Chem. Rev.* **2001**, *101*, 3219–3232; (d) Bouillère, F.; Thétiot-Laurent, S.; Kouklovsky, C.; Alezra, V. *Amino Acids* **2011**, *41*, 687–707.
5. (a) Chatterjee, S.; Roy, R. S.; Balaram, P. *J.R. Soc. Interface* **2007**, *4*, 587–606; (b) Vasudev, P. G.; Chatterjee, S.; Shamala, N.; Balaram, P. *Chem. Rev.* **2011**, *111*, 657–687.
6. (a) Chatterjee, S.; Vasudev, P. G.; Raghothama, S.; Ramakrishnan, C.; Shamala, N.; Balaram, P. *J. Am. Chem. Soc.* **2009**, *131*, 5956–5965; (b) Vasudev, P. G.; Chatterjee, S.; Shamala, N.; Balaram, P. *Acc. Chem. Res.* **2009**, *42*, 1628–1639.
7. (a) Balaram, P. *Biopolymers (Pept. Sci.)* **2010**, *94*, 733–741; (b) Vasudev, P. G.; Chatterjee, S.; Ramakrishnan, C.; Shamala, N.; Balaram, P. *Biopolymers (Pept.Sci.)* **2009**, *92*, 426–435; (c) Vasudev, P. G.; Ananda, K.; Chatterjee, S.; Aravinda, S.; Shamala, N.; Balaram, P. *J. Am. Chem. Soc.* **2007**, *129*, 4039–4048; (d) Guo, L.; Zhang, W.; Reidenbach, A. G.; Giuliano, M. ,W.; Guzei, I. A.; Spencer, L. C.; Gellman, S. H. *Angew. Chem., Int. Ed.* **2011**, *50*, 5843–5846.
8. Guo, L.; Almeida, A. M.; Zhang, W.; Reidenbach, A. G.; Choi, S. H.; Guzei, I. A.; Gellman, S. H. *J. Am. Chem. Soc.* **2010**, *132*, 7868–7869.
9. Pluncinska, K.; Liberek, B. *Tetrahedron* **1987**, *43*, 3509–3517.
10. Seebach, D.; Overhand, M.; Kuhnle, F. N. M.; Martinini, B.; Oberer, L.; Hommel, U.; Widmer, H. *Helv. Chim. Acta* **1996**, *79*, 913–941.
11. Guibourdenche, C.; Seebach, D. *Helv. Chim. Acta* **1997**, *80*, 1–13.
12. Smrcma, M.; Maler, P.; Majerov, E.; Guerassina, T. A.; Eissenstat, M. A. *Tetrahedron* **1997**, *53*, 12867–12874.
13. Schneider, T. R.; Sheldrick, G. M. *Acta Crystallogr.* **2002**, *D58*, 1772–1779.
14. Sheldrick, G. M. *SHELXS-97, A Program for Automatic Solution of Crystal Structures*; University of Göttingen: Göttingen, 1997.
15. Sheldrick, G. M. *SHELXL-97, A Program for Crystal Structure Refinement*; University of Göttingen: Göttingen, 1997.